

A model reduction approach to numerical inversion for a parabolic partial differential equation

Alexander V. Mamonov¹,
Liliana Borcea², Vladimir Druskin³
and Mikhail Zaslavsky³

¹Schlumberger and the University of Texas at Austin (ICES)

²University of Michigan, Ann Arbor

³Schlumberger-Doll Research Center

Support: NSF DMS-0934594.



A model reduction approach to numerical inversion for a parabolic partial differential equation

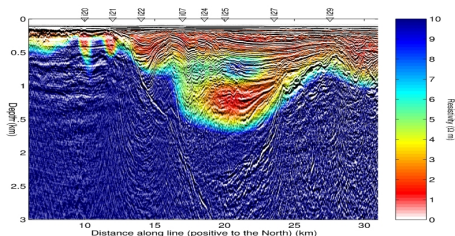
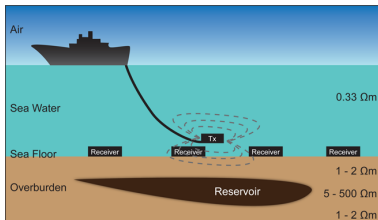
- 1 Problem formulation
- 2 Model order reduction and inversion
- 3 Matching conditions
- 4 Non-linear preconditioner and its Jacobian
- 5 Inversion method and numerical results
- 6 Extension to two dimensions
- 7 Conclusions and future work



Motivation

Problem: Time-domain Controlled Source Electromagnetic (CSEM) method in oil and gas exploration

- Determine the resistivity in the subsurface from time-resolved surface measurements
- Quasi-stationary parabolic Maxwell system
- Highly non-linear inverse problem, local minima, slow convergence
- Expensive forward modeling



Figures from: <http://www.acceleware.com>, <http://www.engineerlive.com/Mining-Engineer/CSEM>



Continuum problem

- Layered medium, one-dimensional equation

$$\frac{\partial}{\partial x} \left[r(x) \frac{\partial u(t, x)}{\partial x} \right] = \frac{\partial u(t, x)}{\partial t}, \quad x \in [0, 1], \quad t > 0$$

- Boundary and initial conditions

$$u_x(t, 0) = u(t, 1) = 0, \quad u(0, x) = \delta(x)$$

- Measurements: boundary time-domain response

$$y(t) = u(t, 0), \quad t > 0$$

- Inverse problem:** given $y(t)$ for $t > 0$ find $r(x)$
- Inverse boundary value problems for parabolic (and elliptic) equations are typically ill-posed
- Ill-posedness in continuum leads to poor conditioning in numerics



Model reduction framework: semi-discrete system

- Discretize on a fine (uniform) grid in space with spacing $h = 1/(N + 1)$

$$\frac{\partial \mathbf{u}(t)}{\partial t} = A(\mathbf{r})\mathbf{u}(t), \quad \mathbf{u}(0) = \frac{1}{h}\mathbf{e}_1 \quad (1)$$

- Discretization of the differential operator

$$A(\mathbf{r}) = -D^T \text{diag}(\mathbf{r})D, \quad \mathbf{r} \in \mathbb{R}_+^N$$

- Time-domain response

$$y(t; \mathbf{r}) = \mathbf{e}_1^T \mathbf{u}(t)$$

- Semi-discrete inverse problem:** given $y(t; \mathbf{r})$ find $\mathbf{r} \in \mathbb{R}_+^N$
- Treat (1) as a dynamical system, apply model reduction techniques
- Model reduction: given \mathbf{r} find a reduced model that approximates y
- “Inverse” model reduction:** obtain a reduced model from the y , then find \mathbf{r} which has this reduced model



Optimization formulation: non-linear preconditioning

- Noisy data

$$d(t) = y(t; \mathbf{r}^{\text{true}}) + \xi(t), \quad t > 0,$$

where $\xi(t)$ is due to noise and discretization errors.

- Optimization formulation**

$$\mathbf{r}^* = \arg \min_{\mathbf{r} \in \mathcal{S}} \frac{1}{2} \|\mathcal{Q}(d(t)) - \mathcal{Q}(y(t; \mathbf{r}))\|_2^2 + \frac{\alpha}{2} \mathcal{P}(\mathbf{r})$$

- Solution method: **Gauss-Newton** or non-linear CG
- Traditional approach: output least squares, no preconditioner \mathcal{Q} , regularization term \mathcal{P} Tikhonov or TV
- Drawbacks: non-convexity, easy to get stuck in local minima, slow convergence, difficulties with high contrast, expensive
- Non-linear preconditioner** $\mathcal{Q} : C(0, +\infty) \rightarrow \mathbb{R}^q$ with small q , the dimension of parameters of reduced models
- The mapping $\mathcal{Q}(y(\cdot; \mathbf{r})) : \mathbb{R}^N \rightarrow \mathbb{R}^q$ is an **approximate identity**



Projection-based model reduction

- Transfer function of the full model $A(\mathbf{r}) \in \mathbb{R}^{N \times N}$, $\mathbf{b} \in \mathbb{R}^N$

$$G(s; \mathbf{r}) = \int_0^{+\infty} y(t; \mathbf{r}) e^{-st} dt = \mathbf{b}^T (sI - A(\mathbf{r}))^{-1} \mathbf{b}, \quad s > 0, \quad \mathbf{b} = \frac{1}{\sqrt{h}} \mathbf{e}_1$$

- Transfer function of a reduced model $A_m \in \mathbb{R}^{m \times m}$, $\mathbf{b}_m \in \mathbb{R}^m$

$$G_m(s) = \mathbf{b}_m^T (sI_m - A_m)^{-1} \mathbf{b}_m$$

- Projection-based model reduction

$$A_m = V^T A V, \quad \mathbf{b}_m = V^T \mathbf{b}, \quad V^T V = I_m$$

- Columns of $V \in \mathbb{R}^{N \times m}$ span the projection **subspace**
- Choice of subspace is dictated by **matching conditions**

$$\left. \frac{\partial^k G_m}{\partial s^k} \right|_{s=\sigma_j} = \left. \frac{\partial^k G}{\partial s^k} \right|_{s=\sigma_j}, \quad j = 1, \dots, m, \quad k = 0, \dots, 2M_j - 1$$

at **interpolation nodes** $\sigma_j \in [0, +\infty)$



Rational Krylov Model Reduction

- Reduced order transfer function admits a partial fraction expansion

$$G_m(s) = \sum_{j=1}^m \frac{c_j}{s + \theta_j}, \quad c_j > 0, \quad \theta_j > 0,$$

with negative **poles** $-\theta_j$ and positive **residues** c_j

- Rational G_m , hence **rational interpolation**
- Typical choices of projection subspaces in model reduction: rational **Krylov** subspaces

$$\mathcal{K}_m(\sigma) = \text{span} \{ (\sigma_j I - A)^{-k} \mathbf{b} \mid j = 1, \dots, m; k = 1, \dots, M_j \}$$

- Popular special cases for **forward** modeling: moment matching

$$\mathcal{K}_m(+\infty) = \text{span} \{ \mathbf{b}, A\mathbf{b}, \dots, A^{m-1}\mathbf{b} \}$$

$$\mathcal{K}_m(0) = \text{span} \{ A^{-1}\mathbf{b}, A^{-2}\mathbf{b}, \dots, A^{-m}\mathbf{b} \}$$

- $\mathcal{K}_m(+\infty)$ is bad for inversion



Inversion via model reduction: \mathcal{H}_2 -optimality

- Proposed in [Druskin, Simoncini, Zaslavsky, 2011]
- Based on \mathcal{H}_2 -optimal reduced models
- View reduced model as a function of interpolation nodes σ

$$y_m(t; \sigma) = \mathbf{b}^T V(\sigma) e^{A_m(\sigma)t} V(\sigma)^T \mathbf{b}, \quad \text{for } A_m(\sigma) = V(\sigma)^T A(\mathbf{r}) V(\sigma)$$

- Minimize time-domain error in L_2 sense

$$\sigma^* = \arg \min \|y(t; \mathbf{r}) - y_m(t; \sigma)\|_{L_2[0, +\infty)}$$

- Equivalent to \mathcal{H}_2 -optimality in Laplace domain (solve with IRKA)

$$\sigma^* = \arg \min \|G(s; \mathbf{r}) - G_m(s)\|_{\mathcal{H}_2}$$

- Use poles and residues of $G_m(s)$ as parameters in inversion
- Define the non-linear preconditioner with a **chain of mappings**

$$\mathcal{Q}_{\mathcal{H}_2}(y(\cdot; \mathbf{r})) : \mathbf{r} \xrightarrow{(a)} A(\mathbf{r}) \xrightarrow{(b)} \sigma^* \xrightarrow{(c)} V(\sigma^*) \xrightarrow{(d)} A_m \xrightarrow{(e)} \{(c_j, \theta_j)\}_{j=1}^m$$



Inversion via model reduction: continued fraction

- We propose a different choice of parameters and matching conditions
- Write the reduced model response as a **continued fraction**

$$G_m(s) = \frac{1}{\hat{\kappa}_1 s + \frac{1}{\kappa_1 + \frac{1}{\ddots + \frac{1}{\hat{\kappa}_m s + \frac{1}{\kappa_m}}}}}$$

- This is a response $w_1(s)$ of a second-order finite difference scheme

$$\frac{1}{\hat{\kappa}_j} \left(\frac{w_{j+1} - w_j}{\kappa_j} - \frac{w_j - w_{j-1}}{\kappa_{j-1}} \right) - s w_j = 0$$

- Continued fraction coefficient are **discrete resistivities**
- Use $\{(\kappa_j, \hat{\kappa}_j)\}_{j=1}^m$ as parameters in inversion, define \mathcal{Q} as a chain

$$\mathcal{Q}(y(\cdot; \mathbf{r})) : \mathbf{r} \xrightarrow{(a)} \mathbf{A}(\mathbf{r}) \xrightarrow{(b)} \mathbf{V} \xrightarrow{(c)} \mathbf{A}_m \xrightarrow{(d)} \{(\mathbf{C}_j, \theta_j)\}_{j=1}^m \xrightarrow{(e)} \{(\kappa_j, \hat{\kappa}_j)\}_{j=1}^m$$



Matching conditions for inversion

- The choice of matching conditions is important: what is good for forward modeling is not necessarily good for inversion
- Use the Jacobian of \mathcal{Q} to quantify the quality of matching conditions

$$(\mathcal{D}\mathcal{Q})_{j,k} = \begin{cases} \frac{\partial \kappa_j}{\partial r_k}, & \text{for } j = 1, \dots, m \\ \frac{\partial \widehat{\kappa}_j}{\partial r_k}, & \text{for } j = m + 1, \dots, 2m \end{cases}, \quad k = 1, \dots, N.$$

- Proper matching conditions should give good **conditioning** and **resolution**
- Good conditioning of $\mathcal{D}\mathcal{Q}$ is desirable for fast and robust performance of Gauss-Newton iteration, possible to achieve $\text{cond}(\mathcal{D}\mathcal{Q}) \approx O(1)$
- Conditioning of $\mathcal{Q}(d(\cdot))$ always grows exponentially (unavoidable ill-posedness), slower growth is preferential
- Resolution is connected to **optimal grids**



Connection to optimal grids

- Optimal (spectrally matched) grids were introduced in [Druskin, Knizhnerman, 2000] for exponential superconvergence of DtN maps
- Typically defined for $r(x) \equiv 1$

$$(\kappa_j^{(0)}, \widehat{\kappa}_j^{(0)})_{j=1}^m = \mathcal{Q}(y(\cdot, \mathbf{r}^{(0)})), \quad \mathbf{r}^{(0)} = (1, 1, \dots, 1)^T$$

- Continued fraction coefficients are the grid steps of FD scheme for

$$\Delta w - sw = 0$$

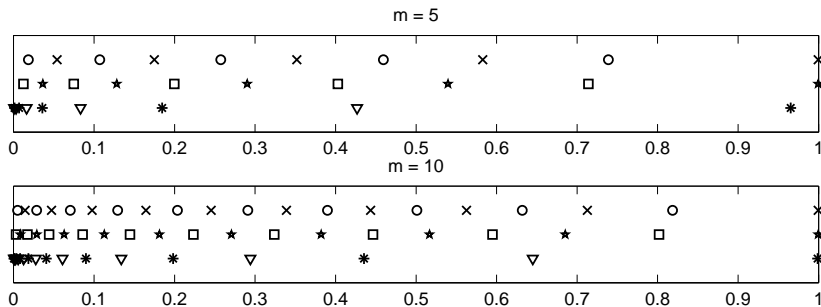
- Staggered grid with primary and dual nodes

$$x_j^{(0)} = \sum_{k=1}^j \kappa_k^{(0)}, \quad \widehat{x}_j^{(0)} = \sum_{k=1}^j \widehat{\kappa}_k^{(0)}, \quad j = 1, \dots, m$$

- Optimal grids were used for inversion (Sturm-Liouville, EIT)
- Here we do not explicitly use optimal grids for inversion, but to quantify the resolution



Optimal grids for different matching conditions

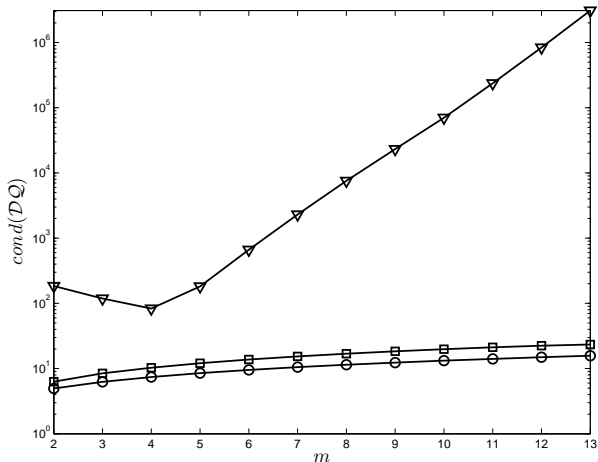


Compare three choices of matching conditions:

- (\circ, \times) Moment matching at zero, $\mathcal{K}_m(0) = \text{span} \{A^{-1}\mathbf{b}, A^{-2}\mathbf{b}, \dots, A^{-m}\mathbf{b}\}$
- (\square, \star) Interpolation $\mathcal{K}_m(\tilde{\sigma}) = \text{span} \{(\tilde{\sigma}_j I - A)^{-1}\mathbf{b} \mid j = 1, \dots, m\}$ at geometrically spaced nodes $\tilde{\sigma}_j = \tilde{\sigma}_1 (1 + C/m)^{j-1}$
- $(*, \nabla)$ Interpolation at fast growing nodes σ^*



Conditioning of the Jacobian



- Rows of \mathcal{DQ} have the meaning of **sensitivity functions**
- Each row corresponds to one grid cell
- Sensitivity functions are localized
- Peak locations are at the optimal grid nodes
- Clustered nodes lead to (almost) linearly dependent rows of \mathcal{DQ}

Condition number growth for moment matching at zero (\circ), interpolation at $\tilde{\sigma}$ (\square), interpolation at σ^* (∇)



Conditioning of rational approximation

- Optimization objective requires computing

$$(\kappa_j, \hat{\kappa}_j)_{j=1}^m = \mathcal{Q}(d(\cdot))$$

- The most **unstable** step in inversion procedure
- Rational approximation (interpolation) problem
- **Simple Padé** for moment matching $\mathcal{K}_m(0)$

$$\left. \frac{\partial^j G_m}{\partial s^j} \right|_{s=0} = \left. \frac{\partial^j G}{\partial s^j} \right|_{s=0} = (-1)^j \int_0^{+\infty} y(t; \mathbf{r}) t^j dt, \quad j = 0, 1, \dots, 2m - 1$$

- **Multipoint Padé** for osculatory interpolation $\mathcal{K}_m(\tilde{\sigma})$

$$G_m(s) = \frac{p(s)}{q(s)}, \quad \begin{cases} p(\tilde{\sigma}_j) - G_m(\tilde{\sigma}_j)q(\tilde{\sigma}_j) = 0 \\ p'(\tilde{\sigma}_j) - G_m'(\tilde{\sigma}_j)q(\tilde{\sigma}_j) - G_m(\tilde{\sigma}_j)q'(\tilde{\sigma}_j) = 0 \end{cases},$$

for $j = 1, \dots, m$

- Once the coefficients of $p(s)$ and $q(s)$ are known, can compute the poles, residues and the continued fraction coefficients easily



Conditioning of rational approximation: comparison

m	2	3	4	5	6
$\text{cond}(T_m)$	$5.28 \cdot 10^1$	$1.26 \cdot 10^5$	$1.84 \cdot 10^9$	$9.14 \cdot 10^{13}$	$2.86 \cdot 10^{16}$
$\text{cond}(R_m)$	$4.43 \cdot 10^2$	$6.73 \cdot 10^4$	$1.85 \cdot 10^7$	$6.95 \cdot 10^9$	$3.83 \cdot 10^{12}$

- Both simple and multipoint Padé problems may be solved via SVD
- Simple Padé: SVD of **Toeplitz** matrix $T_m \in \mathbb{R}^{m \times (m+1)}$ of Taylor coefficients $\tau_j, j = 1, \dots, 2m - 1$ of

$$G(s) = \tau_0 + \tau_1 s + \tau_2 s^2 + \dots + \tau_{2m-1} s^{2m-1} + \dots$$

- Multipoint Padé: SVD of $R_m \in \mathbb{R}^{2m \times (2m+1)}$

$$R_m = \begin{bmatrix} \Sigma_{1:m, 1:m} & -F\Sigma \\ \Sigma'_{1:m, 1:m} & -F'\Sigma - F\Sigma' \end{bmatrix},$$

with **Vandermonde** Σ and $F = \text{diag}(G(\tilde{\sigma}))$

- Multipoint Padé is clearly **superior**



Computing \mathcal{Q} and $\mathcal{D}\mathcal{Q}$: chain of mappings

- Chain of mappings for computing \mathcal{Q} and the Jacobian $\mathcal{D}\mathcal{Q}$

$$\mathcal{Q}(y(\cdot; \mathbf{r})) : \mathbf{r} \xrightarrow{(a)} \mathbf{A}(\mathbf{r}) \xrightarrow{(b)} \mathbf{V} \xrightarrow{(c)} \mathbf{A}_m \xrightarrow{(d)} \{(\mathbf{c}_j, \theta_j)\}_{j=1}^m \xrightarrow{(e)} \{(\kappa_j, \hat{\kappa}_j)\}_{j=1}^m$$

(a) $\mathbf{A}(\mathbf{r}) = -\mathbf{D}^T \text{diag}(\mathbf{r}) \mathbf{D}$, trivial to differentiate.

(b) Requires differentiation of orthonormal basis \mathbf{V} .
Here we differentiate QR decomposition.

(c) $\mathbf{A}_m = \mathbf{V}^T \mathbf{A} \mathbf{V}$, trivial to differentiate once $\mathcal{D}\mathbf{V}$ is known.

(d) Differentiation of eigendecomposition

$$\mathbf{c}_j = (\mathbf{b}_m^T \mathbf{z}_j)^2, \quad \mathbf{A}_m \mathbf{z}_j + \theta_j \mathbf{z}_j = 0, \quad \|\mathbf{z}_j\| = 1, \quad j = 1, \dots, m$$

(e) Lanczos iteration. Explicit differentiation formulas derived in [Borcea, Druskin, Knizhnerman, 2005]

- Steps (d)–(e) can be combined into one using a variant of Lanczos. No explicit formulas, requires differentiation of the iteration.



Differentiation of QR decomposition

- Krylov matrix $K = [(\tilde{\sigma}_1 I - A)^{-1} \mathbf{b}, \dots, (\tilde{\sigma}_m I - A)^{-1} \mathbf{b}] \in \mathbb{R}^{N \times m}$
- Compute V from QR decomposition: $K = VR$, $K^T K = R^T R = LL^T$
- Need to differentiate Cholesky to get

$$\frac{\partial V}{\partial r_k} = \left(\frac{\partial K}{\partial r_k} - V \frac{\partial L^T}{\partial r_k} \right) L^{-T}, \quad k = 1, \dots, N$$

Proposition (Differentiation of Cholesky factorization)

Let $M \in \mathbb{R}^{n \times n}$ be a matrix with Cholesky factorization $M = LL^T$. Given the perturbation δM of M , the corresponding perturbation δL of the Cholesky factor is computed by the following algorithm.

For $k = 1, \dots, n$

$$\delta L_{kk} = \frac{1}{L_{kk}} \left(\frac{\delta M_{kk}}{2} - \sum_{j=1}^{k-1} \delta L_{kj} L_{kj} \right)$$

For $i = k + 1, \dots, n$

$$\delta L_{ik} = \frac{1}{L_{kk}} \left(\delta M_{ik} - \sum_{j=1}^k \delta L_{kj} L_{ij} - \sum_{j=1}^{k-1} \delta L_{ij} L_{kj} \right)$$

Regularization

- Traditional approaches require regularization for stability
- We use regularization only to improve the reconstruction quality
- **Separate** the fitting $\|Q(d(\cdot)) - Q(y(\cdot; \mathbf{r}))\|_2$ step from regularization step
- Jacobian $DQ \in \mathbb{R}^{2m \times N}$ has a **large null space** $2m \ll N$
- Minimize the regularization functional $\mathcal{P}(\mathbf{r})$ in $\text{null}(DQ)$
- Weighted discrete H^1 seminorm

$$\mathcal{P}(\mathbf{r}) = \frac{1}{2} \|W^{1/2} \Delta \mathbf{r}\|_2^2,$$

here Δ is the truncation of D (first derivative, not second)

- Works for both smooth ($W = I$) and piecewise constant resistivities (non-linear re-weighting at every iteration)
- Constrained optimization subproblem at each Gauss-Newton iteration

$$\begin{aligned} & \text{minimize} && \rho^T \Delta^T W \Delta \rho \\ \text{s.t.} & [DQ](\mathbf{r} - \rho) = 0 \end{aligned}$$



Regularization

- Regularization subproblem: quadratic with linear constraints
- First order optimality conditions, **explicit solution** from

$$\begin{aligned} \Delta^T W \Delta \rho + [\mathcal{D}Q]^T \lambda &= 0 \\ [\mathcal{D}Q] \rho &= [\mathcal{D}Q] \mathbf{r} \end{aligned}$$

- May be ill-conditioned, SVD truncation, drop the smallest singular value
- Non-trivial weight ($W \neq I$) is needed for **piecewise constant** resistivities
- Use weight introduced in [Abubakar, Habashy, Druskin, Knizhnerman, Alumbaugh, 2008]

$$w_j = (([\Delta \mathbf{r}]_j)^2 + \phi(\mathbf{r})^2)^{-1}, \quad j = 1, \dots, N-1,$$

where

$$\phi(\mathbf{r}) = C_\phi \|Q(d(\cdot)) - Q(y(\cdot; \mathbf{r}))\|_2$$

- Sharp resolution of interfaces



Inversion algorithm

- 1 Solve the data fitting rational interpolation problem $(\kappa_j^*, \widehat{\kappa}_j^*)_{j=1}^m = \mathcal{Q}(d(\cdot))$
- 2 Work with logarithms $\mathbf{I}^* = (\log \kappa_1^*, \dots, \log \kappa_m^*, \log \widehat{\kappa}_1^*, \dots, \log \widehat{\kappa}_m^*)^T$
- 3 Choose on initial guess $\mathbf{r}^{(1)} \in \mathcal{R}_+^N$
- 4 For $p = 1, \dots, n_{GN}$ do

- 1 Compute the non-linear preconditioner $(\kappa_j^{(p)}, \widehat{\kappa}_j^{(p)})_{j=1}^m = \mathcal{Q}(y(t; \mathbf{r}^{(p)}))$ and its Jacobian $\mathcal{D}\mathcal{Q}^{(p)} = \mathcal{D}\mathcal{Q}(y(t; \mathbf{r}^{(p)}))$
- 2 Work with logs $\mathbf{I}^{(p)} = (\log \kappa_1^{(p)}, \dots, \log \kappa_m^{(p)}, \log \widehat{\kappa}_1^{(p)}, \dots, \log \widehat{\kappa}_m^{(p)})^T$
- 3 Gauss-Newton step

$$\boldsymbol{\rho}^{(p)} = - \left(\mathcal{D}\mathcal{Q}^{(p)} \right)^\dagger \text{diag} \left(\kappa_1^{(p)}, \dots, \kappa_m^{(p)}, \widehat{\kappa}_1^{(p)}, \dots, \widehat{\kappa}_m^{(p)} \right) (\mathbf{I}^{(p)} - \mathbf{I}^*)$$

- 4 Gauss-Newton update $\mathbf{r}^{GN} = \mathbf{r}^{(p)} + \zeta^{(p)} \boldsymbol{\rho}^{(p)}$
- 5 Compute the regularization weight for \mathbf{r}^{GN}
- 6 Solve for next iterate $\mathbf{r}^{(p+1)}$ from

$$\begin{bmatrix} \Delta^T W \Delta & (\mathcal{D}\mathcal{Q}^{(p)})^T \\ \mathcal{D}\mathcal{Q}^{(p)} & 0 \end{bmatrix} \begin{bmatrix} \mathbf{r}^{(p+1)} \\ \boldsymbol{\lambda}^{(p)} \end{bmatrix} = \begin{bmatrix} 0 \\ (\mathcal{D}\mathcal{Q}^{(p)}) \mathbf{r}^{GN} \end{bmatrix}$$



Numerical experiments: setup

- Time stepping over $[0, T_{\max}]$ with N_T steps to compute $\mathbf{y} \in \mathbb{R}^{N_T}$
- Systematic discretization errors even in the absence of noise

$$y_j = y(t_j; \mathbf{r}^{\text{true}}) + \xi^{(s)}(t_j), \quad j = 1, \dots, N_T$$

- Generate the data by adding noise $\mathbf{d} = \mathbf{y} + \xi^{(n)}$
- Noise model

$$\xi^{(n)} = \epsilon \text{diag}(\chi_1, \dots, \chi_{N_T}) \mathbf{y},$$

with independent $\chi_k \in \mathcal{N}(0, 1)$

- Reduced model size m chosen based on noise level ϵ

m	3	4	5	6
ϵ	$5 \cdot 10^{-2}$	$5 \cdot 10^{-3}$	10^{-4}	0 (noiseless)

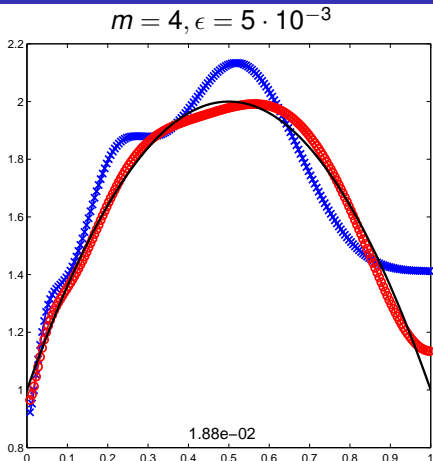
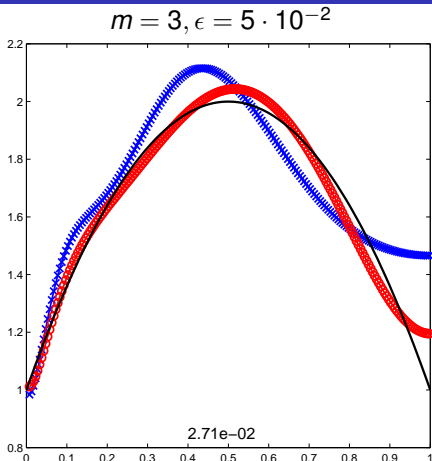
- Relative ℓ_2 error to measure the quality

$$\mathcal{E} = \frac{\|\mathbf{r}^* - \mathbf{r}^{\text{true}}\|_2}{\|\mathbf{r}^{\text{true}}\|_2}$$

- Initial guess $\mathbf{r}^1 = \mathbf{1}$, five Gauss-Newton iterations $n_{GN} = 5$



Numerical results: smooth resistivity

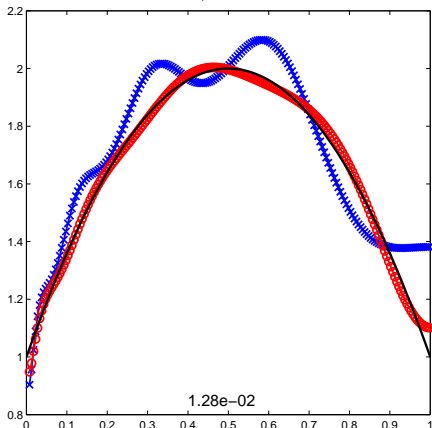


- True resistivity \mathbf{r}^{true} (quadratic)
- × Reconstruction $\mathbf{r}^{(2)}$ after one Gauss-Newton iteration
- Reconstruction $\mathbf{r}^{(6)}$ after five Gauss-Newton iterations

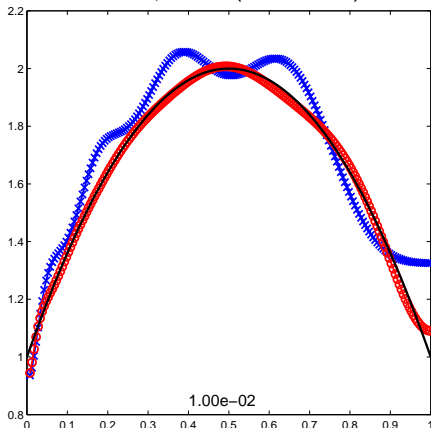


Numerical results: smooth resistivity

$m = 5, \epsilon = 10^{-4}$



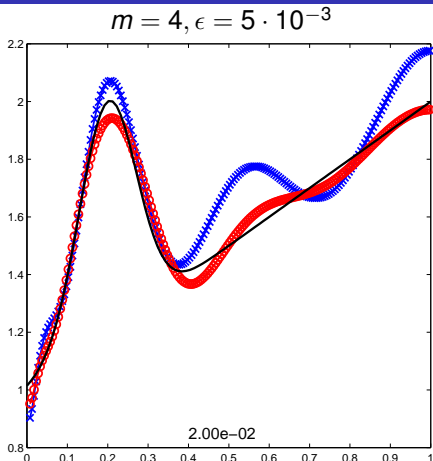
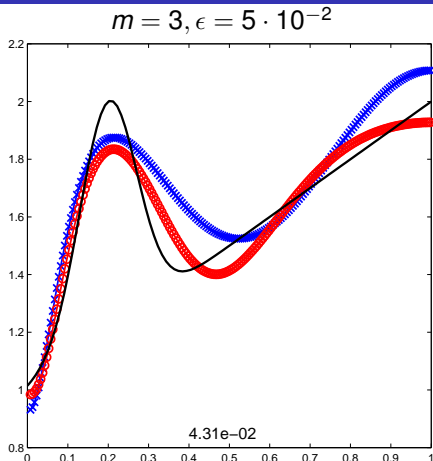
$m = 6, \epsilon = 0$ (noiseless)



- True resistivity \mathbf{r}^{true} (quadratic)
- × Reconstruction $\mathbf{r}^{(2)}$ after one Gauss-Newton iteration
- Reconstruction $\mathbf{r}^{(6)}$ after five Gauss-Newton iterations



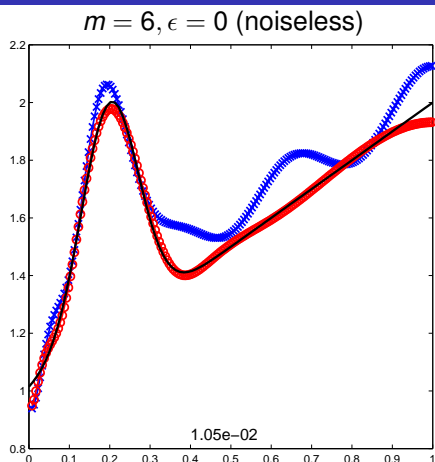
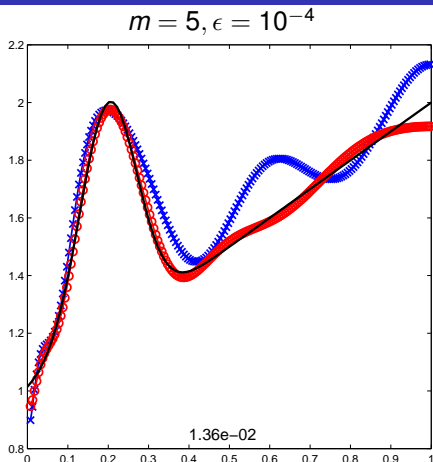
Numerical results: smooth resistivity



- True resistivity \mathbf{r}^{true} (linear + Gaussian)
- × Reconstruction $\mathbf{r}^{(2)}$ after one Gauss-Newton iteration
- Reconstruction $\mathbf{r}^{(6)}$ after five Gauss-Newton iterations



Numerical results: smooth resistivity

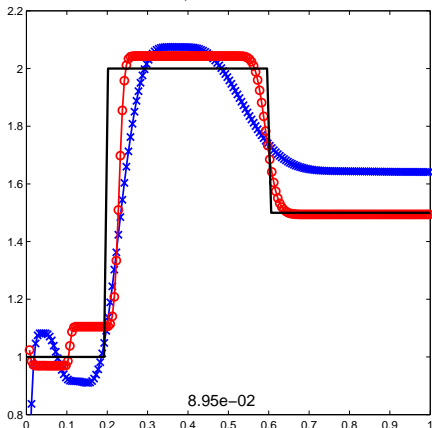


- True resistivity \mathbf{r}^{true} (linear + Gaussian)
- × Reconstruction $\mathbf{r}^{(2)}$ after one Gauss-Newton iteration
- Reconstruction $\mathbf{r}^{(6)}$ after five Gauss-Newton iterations

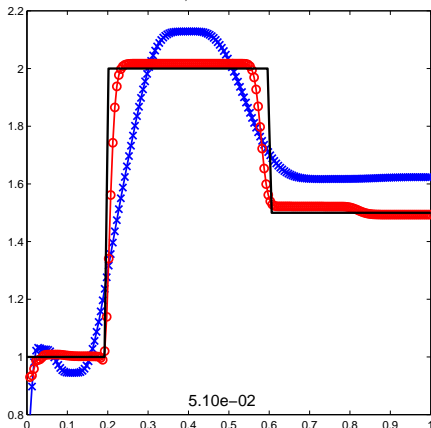


Numerical results: piecewise constant resistivity

$$m = 3, \epsilon = 5 \cdot 10^{-2}$$



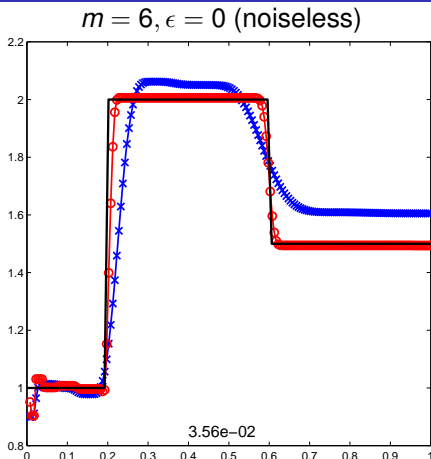
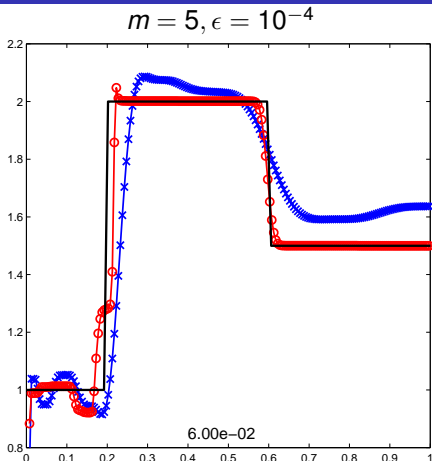
$$m = 4, \epsilon = 5 \cdot 10^{-3}$$



- True resistivity \mathbf{r}^{true} (jump of contrast 2)
- × Reconstruction $\mathbf{r}^{(2)}$ after one Gauss-Newton iteration
- Reconstruction $\mathbf{r}^{(6)}$ after five Gauss-Newton iterations



Numerical results: piecewise constant resistivity



- True resistivity \mathbf{r}^{true} (jump of contrast 2)
- × Reconstruction $\mathbf{r}^{(2)}$ after one Gauss-Newton iteration
- Reconstruction $\mathbf{r}^{(6)}$ after five Gauss-Newton iterations



Approaches to higher dimensions

Higher dimensions:

- One-dimensional problem is formally determined: 1D unknown $r(x)$ and 1D data $y(t)$
- In dimension two the problem is already **overdetermined**: 2D unknown $r(x, y)$, but 3D data $y_{i,j}(t)$, where (i, j) are source-detector pairs
- Straightforward generalization: block Lanczos, block Krylov subspaces, matrix-valued continued fractions
- Block tridiagonal matrix with **dense** blocks, consequence of an overdetermined problem
- Dense blocks do not correspond directly to a finite-difference scheme
- Work with a subset of the data, make the problem formally determined



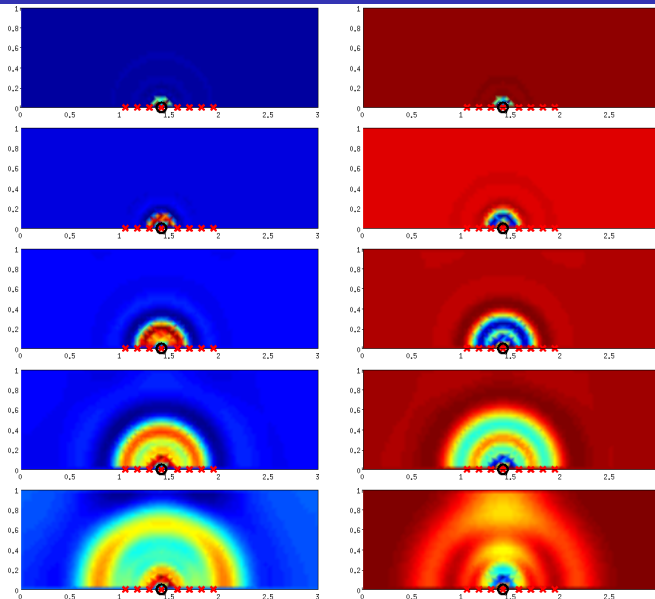
Coinciding sources and receivers (transducers)

Using one scalar continued fraction per transducer:

- Simplest reduction of the data $y_{i,j}(t)$: take the diagonal $i = j$
- Sources and receivers coincide
- Excite at a point on the boundary at $t = 0$, measure $y_j(t)$ at the same location for $t > 0$ for each transducer $j = 1, \dots, n$
- Not the best setting in practice, measurements at source locations may be noisy
- Easier to work with theoretically, coinciding sources/receivers preserve the symmetry
- Construct separate scalar continued fractions interpolating each $y_j(t)$, $j = 1, \dots, n$
- Continued fractions are again Stieltjes due to the symmetry



Sensitivities

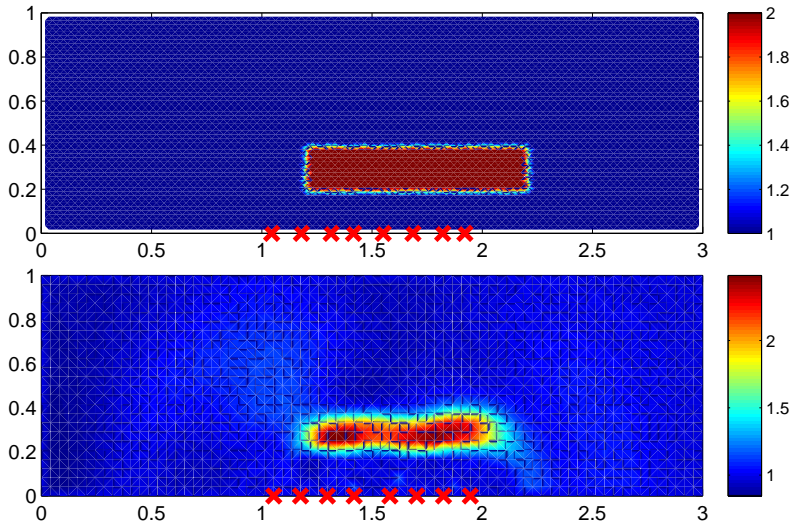


Sensitivity functions of $\widehat{\kappa}_j$ (left) and κ_j (right) for $j = 1, \dots, m$ (top to bottom), $m = 5$ for a single transducer (black \circ) out of $n = 8$ (red \times).

Simple Pade approximant at $\sigma = 60$. Sensitivities resemble propagating spherical waves. Higher σ means lower speed of propagation. Should avoid reflections from boundaries.



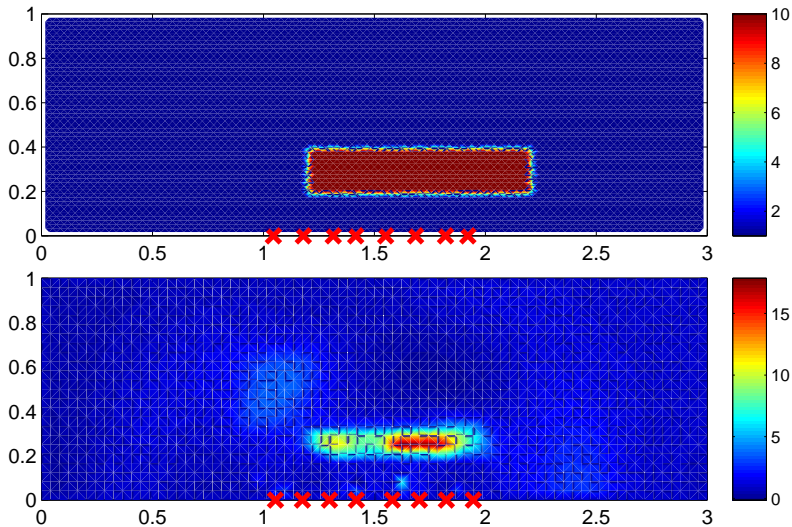
Reconstructions: single low contrast inclusion



Top: true $r(x, y)$. Bottom: reconstruction after a single Gauss-Newton iteration. Constant initial guess $r_0(x, y) \equiv 1$. Transducers: red \times .



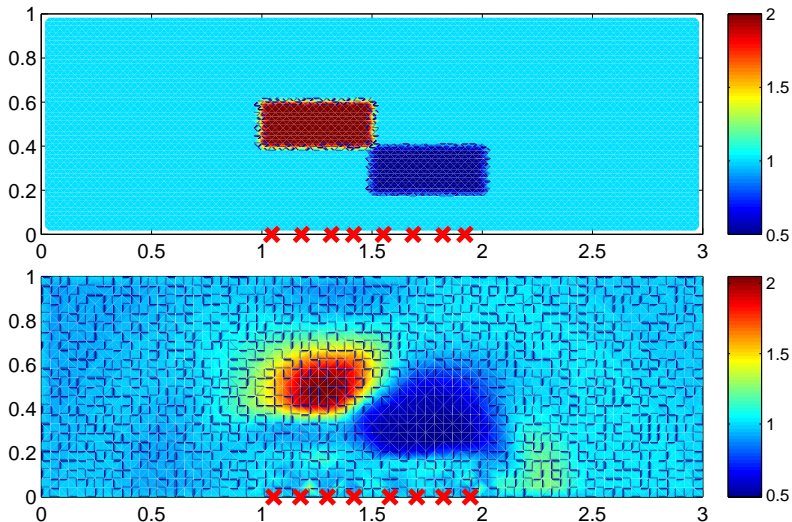
Reconstructions: single high contrast inclusion



Top: true $r(x, y)$. Bottom: reconstruction after a single Gauss-Newton iteration. Constant initial guess $r_0(x, y) \equiv 1$. Transducers: red \times .



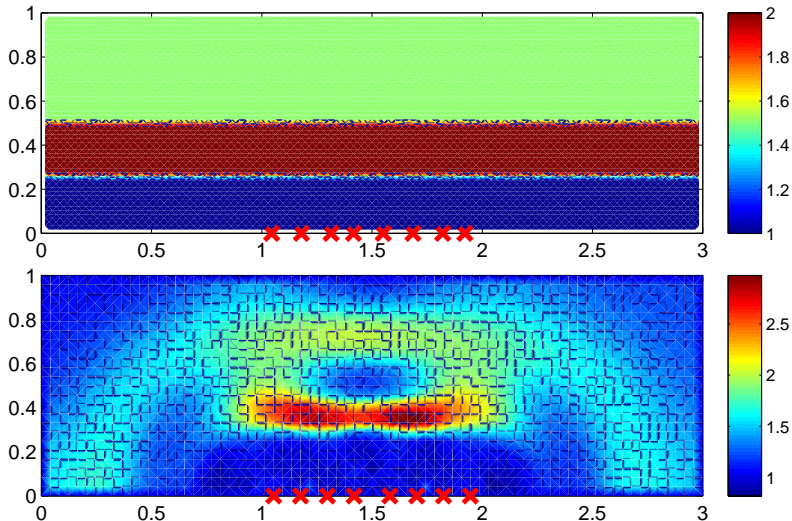
Reconstructions: two adjacent inclusions



Top: true $r(x, y)$. Bottom: reconstruction after a single Gauss-Newton iteration. Constant initial guess $r_0(x, y) \equiv 1$. Transducers: red \times .



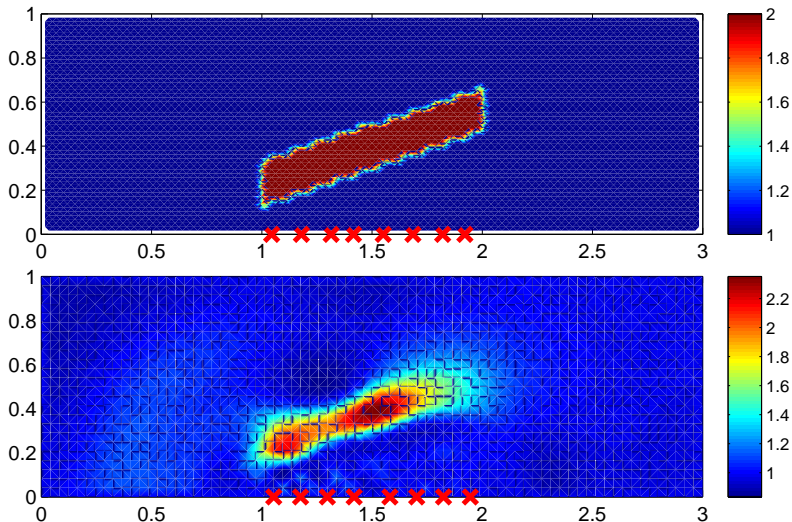
Reconstructions: layered medium



Top: true $r(x, y)$. Bottom: reconstruction after a single Gauss-Newton iteration. Constant initial guess $r_0(x, y) \equiv 1$. Transducers: red \times .



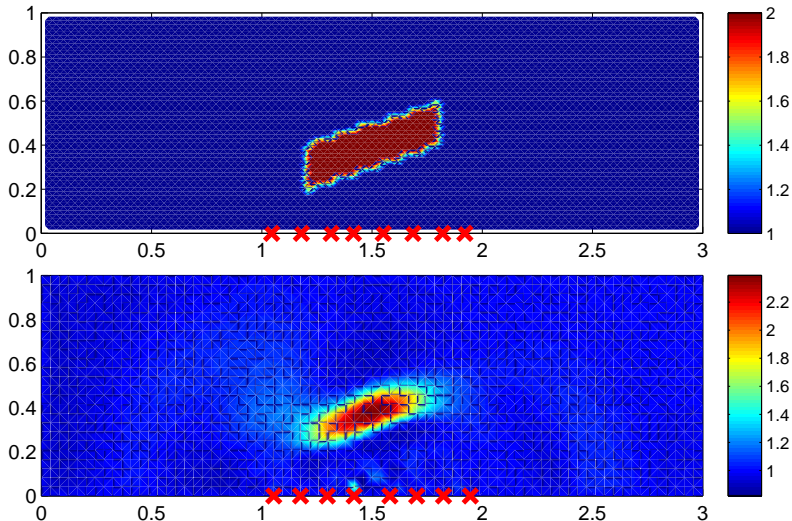
Reconstructions: skewed inclusion, low aperture



Top: true $r(x, y)$. Bottom: reconstruction after a single Gauss-Newton iteration. Constant initial guess $r_0(x, y) \equiv 1$. Transducers: red \times .



Reconstructions: skewed inclusion, high aperture



Top: true $r(x, y)$. Bottom: reconstruction after a single Gauss-Newton iteration. Constant initial guess $r_0(x, y) \equiv 1$. Transducers: red \times .



Conclusions and future work

Conclusions:

- Non-linear preconditioning based on model reduction
- Data fitting: rational interpolation (unavoidably ill-conditioned)
- Reconstruction: well-conditioned
- Fast convergence, inexpensive
- Possible to extend to higher dimensions

Future work:

- More work on 2D and 3D
- Non-coinciding source-receiver pairs
- Deal with the loss of symmetry

Preprint: *A model reduction approach to numerical inversion for a parabolic partial differential equation.* L. Borcea, V. Druskin, A.V. Mamonov and M. Zaslavsky, 2012, arXiv:1210.1257 [math.NA]

